



# *Cocos nucifera* Leaf Extract Mediated Green Synthesis of Silver Nanoparticles for Enhanced Antibacterial Activity

A. K. M. Royhan Uddin<sup>1</sup> · Md. Abu Bakar Siddique<sup>2</sup> · Farjana Rahman<sup>1</sup> · A. K. M. Atique Ullah<sup>3,4</sup> · Rahat Khan<sup>5</sup>

Received: 30 November 2019 / Accepted: 12 March 2020 / Published online: 18 March 2020  
© Springer Science+Business Media, LLC, part of Springer Nature 2020

## Abstract

Antibiotic resistance is currently a global human health concern and insists on the importance of the production of new, alternative and most effective antibiotics. Nano-sized trace metals such as silver nanoparticles (AgNPs) is a potential material with antibacterial properties and hence the synthesis of this material is of considerable interest to the scientific community mainly for antimicrobial applications. In this work, we have successfully green synthesized the AgNPs using *Cocos nucifera* leaf aqueous extract as the natural reducing and stabilizing agent, and aqueous silver nitrate ( $\text{AgNO}_3$ ) solution as a precursor by a newly developed technique. The material was characterized by ultraviolet–visible (UV–Vis) spectrophotometry, X-ray diffractometry (XRD), Fourier transform infrared (FT-IR) spectroscopy, and transmission electron microscopy (TEM) analyses; and subsequently, evaluated their potential candidacy as antibacterial agents against some common human pathogens by the standard disc diffusion method. The synthesized AgNPs were identified by XRD analysis as a cubic crystal system with an average crystallite size of 14.2 nm. The aqueous colloidal suspension of AgNPs shows a UV–Vis absorption maxima of 380 nm indicating its formation. FT-IR analysis identified the C–N, –OH and N–H as the major and probable functional groups in the leaf extract responsible for the production of stable AgNPs. The results of antibacterial studies of the material showed the considerable zones of inhibition against both Gram-positive (*Staphylococcus aureus* and *Bacillus subtilis*) and Gram-negative (*Salmonella typhimurium*, *Escherichia coli*, *Pseudomonas aeruginosa*, and *Citrobacter freundii*) bacteria ranging from 10 to 20 mm with less inhibition for the former than the latter. The maximum (20 mm) and minimum (10 mm) inhibition zone was shown by *C. freundii* and *Bacillus subtilis*, respectively and *P. aeruginosa* shows the second-highest zone of inhibition (19 mm). The antibacterial performance of the material implies that the *C. nucifera* leaf extract mediated green synthesized AgNPs can be regarded as a potential candidate for antimicrobial application appreciably.

---

✉ Md. Abu Bakar Siddique  
sagor.bcsir@gmail.com

<sup>1</sup> Department of Chemistry, Comilla University, Comilla 3506, Bangladesh

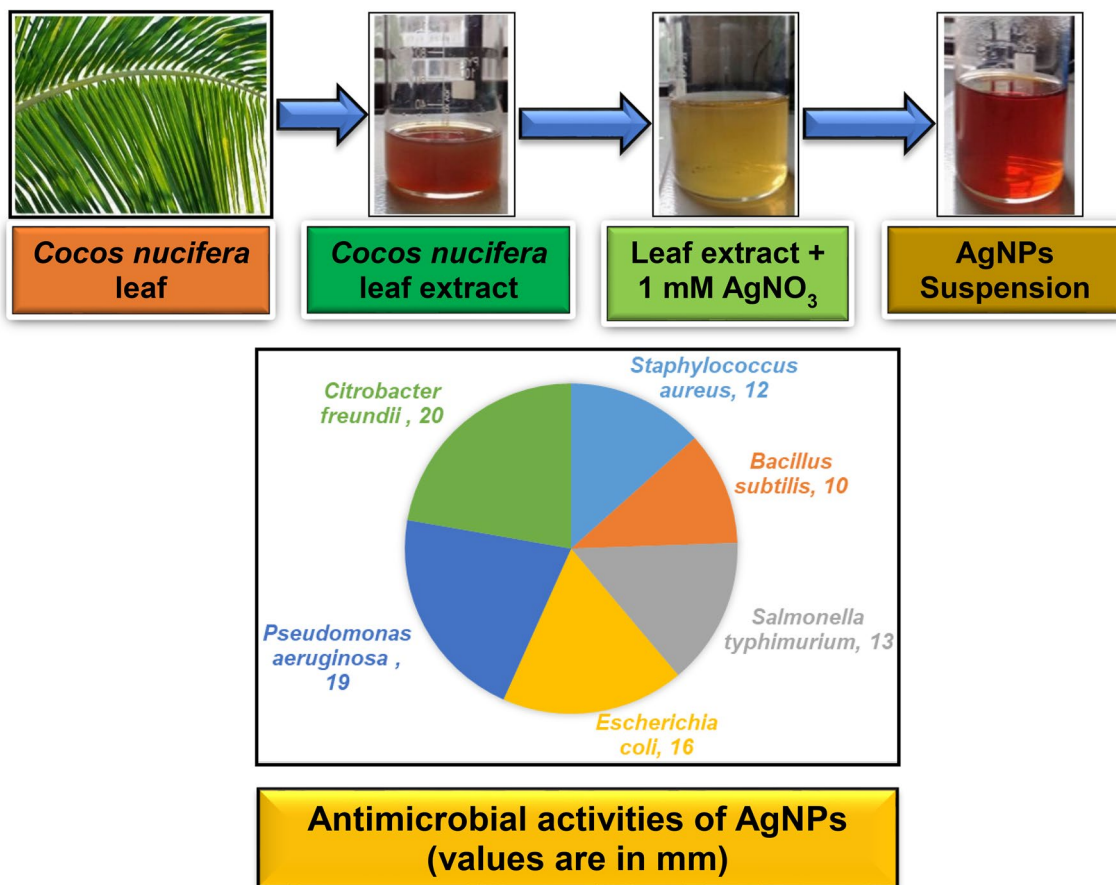
<sup>2</sup> Institute of National Analytical Research and Service (INARS), Bangladesh Council of Scientific and Industrial Research (BCSIR), Dhanmondi, Dhaka 1205, Bangladesh

<sup>3</sup> Analytical Chemistry Laboratory, Chemistry Division, Atomic Energy Centre, Bangladesh Atomic Energy Commission, Dhaka 1000, Bangladesh

<sup>4</sup> Nanoscience and Technology Research Laboratory, Atomic Energy Centre, Bangladesh Atomic Energy Commission, Dhaka 1000, Bangladesh

<sup>5</sup> Institute of Nuclear Science and Technology, Bangladesh Atomic Energy Commission (BAEC), Savar, Dhaka 1349, Bangladesh

## Graphic Abstract



**Keywords** Silver nanoparticles · *Cocos nucifera* leaf extract · Green synthesis · Antibacterial activity · Human pathogens

## 1 Introduction

Antibiotic resistance in the human body is currently an important human health issue [1, 2]. This imparts a substantial interest to the scientific community to develop new, alternative and more effective antimicrobial substances using varieties of precursors. Nanomaterials with antimicrobial properties, for instance, silver nanoparticles (AgNPs) in this regard, can function as a potential candidate to be used as an effective antimicrobial agent in a single or combined form with several suitable substances including commercial antibiotics [3–6]. The potentiality of AgNPs as an antimicrobial activity is well established in wound healing [7]. Furthermore, due to their smaller particle size (1–100 nm), AgNPs have unique properties and attributes. The small size of this material facilitates the enhancement of its physical, chemical, optical and magnetic properties and makes the AgNPs more susceptible to the human pathogen [1, 8]. In addition to the most

important and well-known antibacterial activities against a broad scope of Gram-positive and Gram-negative bacteria, the chemically stable AgNPs can also function as antiviral, antifungal, anti-infection, anti-inflammatory, anti-decay, antiseptic and tranquilizers conveyance agent [9, 10]. AgNPs are also successfully employed for the diagnosis and treatment of cancer and to cure several skin diseases such as abrasions, warts, etc. [11, 12]. Extensive and non-prescribed use of antibiotics over a course of time can develop a resistance to it in the human body. However, AgNPs do not create any resistance in the microorganisms and are easily killed them indicating the betterment of AgNPs. These NPs can act as an effective lethal agent even against some antibiotic-resistant microorganisms [13].

Therefore, the synthesis of AgNPs is of remarkable triumph for biological applications, particularly as an antimicrobial agent. AgNPs having antibacterial activities are also widely applied in medicine, pharmacology, foodstuffs, textile coatings, wound dressings, cleaning

agents, cosmetics and topical ointments [14–19]. It promotes safe to use in dietary supplements, food packaging, and anti-acne preparation. However, recently an enormous use of antibacterial AgNPs in cosmetics (~12%) [20, 21] are threatening to human health as some research showed that AgNPs at a very small range of 0.2–2% can be penetrated through the human skin with the poor skin barrier capacity and can induce a little toxicity to organisms [22, 23]. Long-term uses of AgNPs have an adverse impact on epigenetic dysregulation and gene expression reprogramming [24]. However, AgNPs synthesized using plant extract mediated green approach are not hazardous to the environment [10, 25]. In spite of its wide applications, the evidence for the toxicity of AgNPs synthesized by this approach is still not visible. The bactericidal activity of AgNPs without any toxicity to human and animal cells make them a potential candidate and a suitable substitution for antibiotics [26, 27]. Hence, it is worthwhile to establish a suitable synthesis method of AgNPs having less toxicity with high antibacterial activity for the safe use of them in terms of human health concerns.

The antimicrobial activity of AgNPs depends on the particle dimension and in general, AgNPs with smaller particle dimension shows more antimicrobial effect [3, 8]. Consequently, the size-controlled synthesis of AgNPs is of a tremendous challenge to the researcher [10, 28, 29]. Although a number of physical and chemical methods for the synthesis of AgNPs are available [30–33] green approach synthesis is the most preferable since it has low toxicity impact, fewer biological hazards and smaller energy consumption [1, 34, 35]. Hydrothermal and solvothermal techniques for the AgNPs synthesis involves high temperature and pressure and needs special instrumentation [36–38]. Moreover, the solvothermal process involving the non-aqueous solution may require toxic organic solvents to carry out the chemical reactions [36]. Both these processes sometimes necessitate the use of additives, surfactants and other chemical reagents that are hazardous to the environment and in most cases, difficult to remove from the final product [39, 40]. In this regard, the green approach synthesis method has become more attractive nowadays, since this is easier, eco-friendly, cost-effective and nontoxic in nature [1, 35, 41, 42]. Thus, green synthesis of AgNPs using leaf extract of plants containing the reducing as well as stabilizing agents might be a potential candidate in this regard [43]. In fact, a large number of researchers have synthesized AgNPs with various sizes using several plant extracts mediated green approach [9, 10, 44–46] and utilized the material mostly in antimicrobial and antifungal applications [1–4, 6, 14, 15, 47–69].

Raj and Arulmozhi [70], Mariselvam et al. [71], and Govarthanan et al. [72] synthesized AgNPs using the flower, inflorescence and oil cake extract of *Cocos nucifera*, respectively for antibacterial activity. Gomathi et al.

[73] synthesized AgNPs from *C. nucifera shell* for dengue vector toxicity, detoxification of enzymatic activity and for the predatory response of aquatic organism while Paul et al. [28] used *C. nucifera Linn shell* extract for the synthesis of poly-shaped gold nanoparticles for application in catalysis process. Roopan et al. [74] synthesized AgNPs using *coir* extract of *C. nucifera* for larvicidal activity while Babu et al. [75] and Elumalai et al. [76] used the *Coconut water* for the synthesis of gold and AgNPs, respectively. However, to the best of our knowledge, no work regarding the synthesis of AgNPs using *C. nucifera* leaf extract have been reported earlier. *C. nucifera*, a naturally available species on Earth is commonly known as the “coconut tree”. It belongs to *Arecaceae* family and is mainly cultured in the tropical regions (Bangladesh, India, Sri Lanka, Indonesia, Malaysia, Philippines, so on) having regular rainfall, high humidity and it grows mostly in the sandy soil [77]. The phytochemical screening of *C. nucifera* showed the presence of alkaloids, glycosides, steroids, flavonoids, phenols and terpenoids which are mostly known to have antioxidant properties [77–79].

In this work, AgNPs were green synthesized via a simple and facile synthetic route using *C. nucifera* leaf extract and characterized using several instrumental techniques such as UV–Vis spectrophotometry, XRD, FT-IR, and TEM. The efficacy of the material as a potential candidate for an antimicrobial agent was then justified against some common Gram-positive (two) and Gram-negative (four) human pathogenic bacteria. The Gram-positive species were *Staphylococcus aureus* and *B. subtilis* while the Gram-negative species were *Salmonella typhimurium*, *Escherichia coli*, *Pseudomonas aeruginosa*, and *C. freundii*. *S. aureus*, a human pathogen, generally colonized in the groin, gastrointestinal tract, and axillae [80]. *B. subtilis* strains affect the intestinal function and inflammatory response in broiler chickens [81]. *S. typhimurium* is responsible for intestinal disease in its host including humans [82]. *E. coli* is a very common microorganism exists abundantly on the surface of the mammal’s body creating several infections and is also responsible for potential biological contamination of drinking water [83]. *P. aeruginosa* is found widely in soil, water, and plants and can be regarded as a biomarker of bronchiectasis severity [84, 85]. This affects patients with lung defenses such as cystic fibrosis and pulmonary disease [86, 87]. *C. freundii* is associated with gastroenteritis, neonatal meningitis, septicemia and brain abscess [88, 89].

To the best of our knowledge, we reported for the first time a simple route for the green synthesis of AgNPs using *C. nucifera* leaf extract with a view to applying against the considered bacteria. The work will obviously add to the justification of previously published reports on green synthesis of AgNPs using the leaf extract of several plants.

## 2 Materials and Methods

### 2.1 Materials

The fresh leaves of *C. nucifera* (coconut tree) were collected from the local area of Bangladesh (North Chartha, Comilla). Analytical grade silver nitrate ( $\text{AgNO}_3$ ) was purchased from Fluka Analytical, Sigma-Aldrich, Germany. Bactotrypton, bacto agar, and yeast extract were purchased from HiMedia Laboratories Pvt. Ltd., Mumbai, India. All chemicals and reagents were used as received without further purifications. The deionized (DI) water with electrical conductivity and resistivity of  $0.2 \mu\text{S}/\text{cm}$  and  $18.2 \text{ M}\Omega \text{ cm}$  at  $25 \text{ }^\circ\text{C}$ , respectively were used throughout the experiment.

### 2.2 Preparation of *C. nucifera* Leaf Extract

Prior to the experiment, the collected fresh and healthy leaves of *C. nucifera* were washed several times with tap water followed by DI water to remove inherent unwanted dust particles and debris, and they were cut into small pieces with a sharp knife. The clean pieces of leaves were then sun-dried for a week, oven-dried at  $60 \text{ }^\circ\text{C}$  for 24 h and ground well to form a homogenous powder. About 10 g of finely grounded powder leaves were taken in a 250 mL beaker containing 100 mL of DI water by weighing in a highly precise calibrated digital electrical balance (Model: GR-200, A&D Company Limited, Tokyo, Japan) and boiled at  $80 \text{ }^\circ\text{C}$  for about 20 min. Then, the leaves suspension was incubated for 30 min and the extract was filtered with Whatman™

qualitative 1 filter paper (125 mm dia. \*100 circles), and finally preserved at  $4 \text{ }^\circ\text{C}$  [1] for further experiments. This leaf extract solution was used for the reduction of silver ions ( $\text{Ag}^+$ ) to silver nanoparticles ( $\text{Ag}^0$ ). The schematic representation of the preparation of *C. nucifera* leaf aqueous extract is shown in Fig. 1.

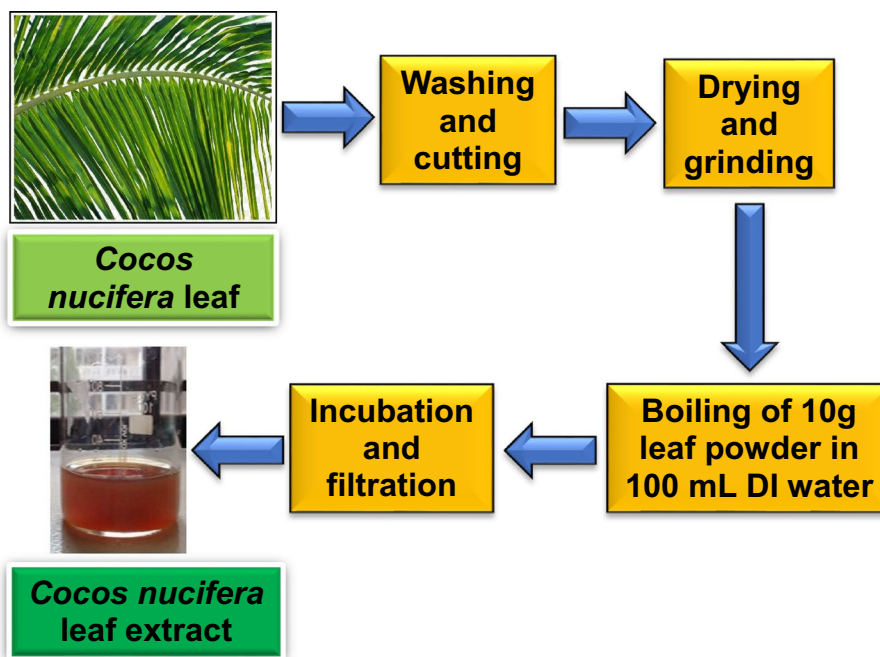
### 2.3 Synthesis of Silver Nanoparticles (AgNPs)

The synthesis of AgNPs was carried out following our previous report [1] with some modification. In brief, 10 mL of *C. nucifera* leaf extract was added dropwise into 90 mL of the aqueous solution of 1 mM  $\text{AgNO}_3$  under vigorous magnetic stirring at room temperature. The solution mixture was then heated at about  $60 \text{ }^\circ\text{C}$  for 30 min for the reduction of  $\text{Ag}^+$  ions to  $\text{Ag}^0$  (formation of AgNPs) indicating with a color change of the solution from greenish orange to dark red after 20 min forming a colloidal suspension (Fig. 2). The suspension was cooled at room temperature ( $30 \text{ }^\circ\text{C}$ ) and centrifuged at 3000 rpm for 15 min to obtain the solid product. The product was washed several times with DI water to remove unreacted nitrate ions and other chemical species in the extract. It was then dried at  $60 \text{ }^\circ\text{C}$  in an electric oven, ground in a quartz mortar with a pestle, collected in a plastic sample vial and stored in a desiccator for further analyses.

### 2.4 Characterization of the Synthesized AgNPs

The ultraviolet–visible (UV–Vis) spectrum of the resulting colloidal suspension of the expected AgNPs was recorded using a UV–Vis spectrophotometer (Model: UV-1650PC,

**Fig. 1** Schematic diagram for the preparation of *Cocos nucifera* leaf extract





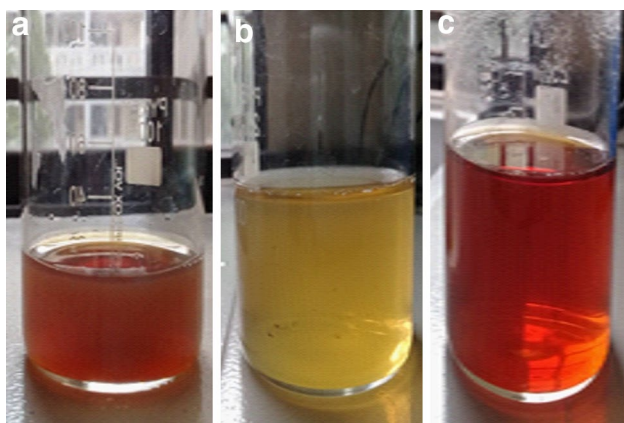


**Fig. 2** **a** *C. nucifera* leaf extract (reddish green), **b** 1 mM AgNO<sub>3</sub> with *C. nucifera* leaf extract (greenish orange), **c** silver nanoparticles (AgNPs) suspension after reaction of 1 mM AgNO<sub>3</sub> with *C. nucifera* leaf extract (dark red)

Shimadzu, Japan) in the wavelength range of 350–500 nm, using DI water as a reference blank for baseline adjustment [1]. The crystalline phase and surface morphology of the AgNPs were studied by X-ray diffraction (XRD) analysis and transmission electron microscopy (TEM), respectively. XRD analysis was conducted using an X-ray powder diffractometer (GBC EMMA, Australia) equipped with monochromatic CuK $\alpha$  radiation (1.5418 Å). The spectra were recorded at 30 kV and 20 mA in the continuous mode with a scan speed of 2.0°/min and scan width of 0.02° within the scan range of 30°–90°. The crystallite size (D) of the prepared AgNPs was calculated from the XRD patterns using the Debye–Scherrer formula [6],  $D = k\lambda/\beta \cos\theta$  where k is a dimensionless shape factor (typical value 0.9),  $\lambda$  is the X-ray wavelength used as the primary beam of Cu-K $\alpha$  ( $\lambda = 1.5418$  Å),  $\beta$  is the line broadening at halfway of the maximum intensity or Full Width at Half Maximum (FWHM) in radian and  $\theta$  is the Bragg's angle of the incident in degree. Fourier transform infrared spectroscopy (FT-IR) was used to identify the existence of inherent functional groups in AgNPs from the biomolecules present in the *C. nucifera* leaf extract. FT-IR spectra were recorded using an FT-IR spectrophotometer (Model: IRAffinity-1S, Shimadzu, Japan) in the mid-IR region (4000–400 cm<sup>-1</sup>). For taking the FT-IR spectra, the dry solid powder of AgNPs (1% w/w) was homogeneously mixed with pure and dry KBr powder in a quartz-mortar by a pestle and compressed mechanically in a metal holder under a pressure of 8–10 tons to make a translucent pellet. The resultant pellet was then placed in the path of the IR beam of the instrument with a sample holder for spectral measurement. Before taking the spectra of the sample, instrumental background measurement was performed and the baseline of the spectrum was adjusted using KBr. The surface morphology of the AgNPs was studied by transmission electron

microscope (TEM) (Model: JEOL, JEM 2010, Japan) applying an acceleration voltage of 120 kV.

## 2.5 Procedure for Antibacterial Activity Studies of AgNPs

The disc diffusion method was employed for assessing the antibacterial activity of the synthesized AgNPs. Six common varieties of bacteria such as *S. aureus* (ATCC 12228), *B. subtilis* (ATCC 6633), *S. typhimurium* (ATCC 14028), *E. coli* (ATCC 25922), *P. aeruginosa* (ATCC 9027) and *C. freundii* (ATCC 8090) were considered for the antibacterial potentiality study of the AgNPs. The bacteria were cultured in Luria Broth (LB) medium (tryptone 1.5%, yeast extract 0.75%, sodium chloride 1.2%) at 37 °C with a 60 rpm shaking water bath [90]. For the study, 20 mL of cooled LB medium was poured into a Petri dish of 10 cm sized and 50 mL of bacteria containing medium was poured on the Petri dish and daubed well with a glass spoon. A filter paper was cut into a number of pieces of about 6 mm size disc and sterilized. These papers were soaked with 20  $\mu$ L of 30 mg/L AgNPs suspensions and placed on the culture dish and incubated at 37 °C for 24 h. For the control study, DI water and *C. nucifera* leaf extract soaked disc was also placed on the dish. After the studied time period, the zones of inhibition in the diameter produced by the tested AgNPs along with the control in each disc were measured carefully in millimeters using a Hi-Media Laboratories Pvt. Ltd. zone scale. The measurements were repeated three times for each sample and mean values of zone diameter with their standard deviations were considered.

## 3 Results and Discussion

### 3.1 Characterization of AgNPs

Primarily, the formation of AgNPs was confirmed by color identifications. During the experiment, the appearance of dark red color suspension from the initial greenish orange color indicates the formation of AgNPs mediated with *C. nucifera* leaf extract (reddish green) (Fig. 2a–c). Then, the synthesis of expected AgNPs was further ensured by several instrumental techniques such as UV–Vis spectrophotometry, XRD, FT-IR, and TEM.

#### 3.1.1 UV–Vis Spectroscopy Studies

Figure 3 shows the UV–Vis spectrum of the colloidal suspension of the reaction mixture of the *C. nucifera* leaf extract and aqueous AgNO<sub>3</sub> solution. The absorption peak appeared at 380 nm in the spectrum may be corroborated to the formation of AgNPs and is due to the surface Plasmon resonance

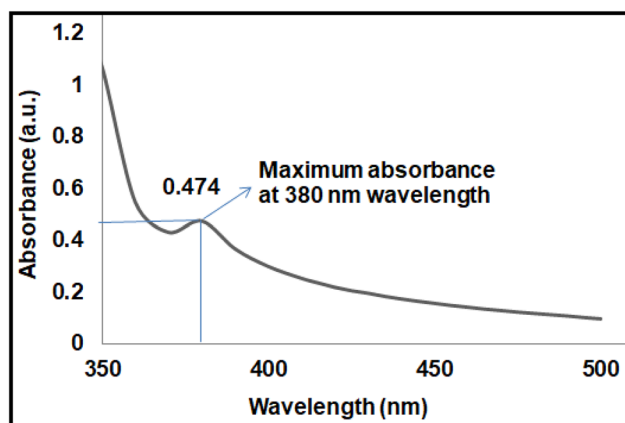


Fig. 3 UV-Vis spectrum of silver nanoparticles

[47, 56, 70, 91–93]. This indicates an optically active nature of the prepared colloidal suspension (Fig. 2c) and the material could be speculated to be AgNPs [1, 91]. No absorption peak was found for aqueous  $\text{AgNO}_3$  solution. From the results of UV-Vis spectrum, it can be concluded that AgNPs were successfully synthesized from the reaction of aqueous solution of  $\text{AgNO}_3$  and *C. nucifera* leaf extract and the color change from greenish orange to dark red might be due to the reduction of the  $\text{Ag}^+$  ion to  $\text{Ag}^0$ , which is correlated with the vibration of the excitation of the surface Plasmon resonance showing the spectroscopic phenomenon of the formation of AgNPs [67, 68, 94].

### 3.1.2 Structural Studies by X-Ray Diffraction (XRD) Analysis

The formation of AgNPs using *C. nucifera* leaf extract was further confirmed by the characteristic patterns observed in XRD analysis (Fig. 4). The XRD patterns showed five diffraction peaks at the  $2\theta$  values of  $38.17^\circ$ ,  $44.37^\circ$ ,  $64.52^\circ$ ,  $77.42^\circ$ , and  $81.52^\circ$  which corresponded to the (111), (200), (220), (311), and (222) planes, respectively. The corresponding phase is identified as cubic Ag crystal system (ICDD Card No. 00–004-0783) with space group:  $\text{Fm}\bar{3}m$  (225), unit cell volume: 68.2, and unit cell parameters:  $a = b = c = 4.09 \text{ \AA}$  and  $\alpha = \beta = \gamma = 90^\circ$ . Moreover, our obtained XRD pattern is very much comparable with previous studies [1, 6, 73, 95]. The average estimated size of the NPs as calculated from the XRD pattern using the Debye–Scherrer formula was found to be 14.2 nm with a range from 12.1 to 16.6 nm.

### 3.1.3 Chemical Analysis by Fourier transform Infrared Spectroscopy (FT-IR)

FT-IR analysis was performed to identify the functional groups present in the *C. nucifera* leaf extract which are

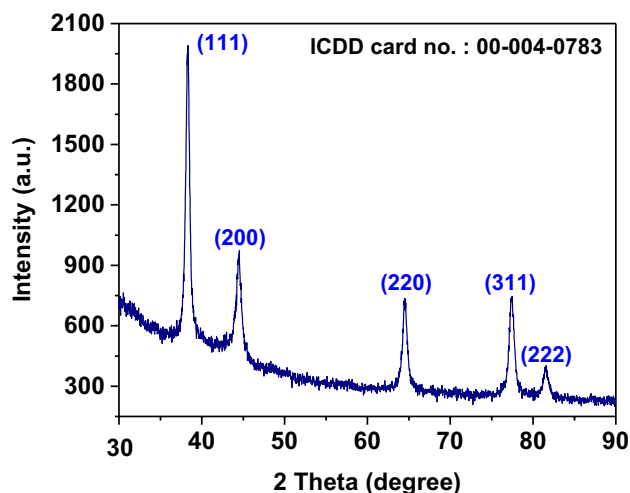
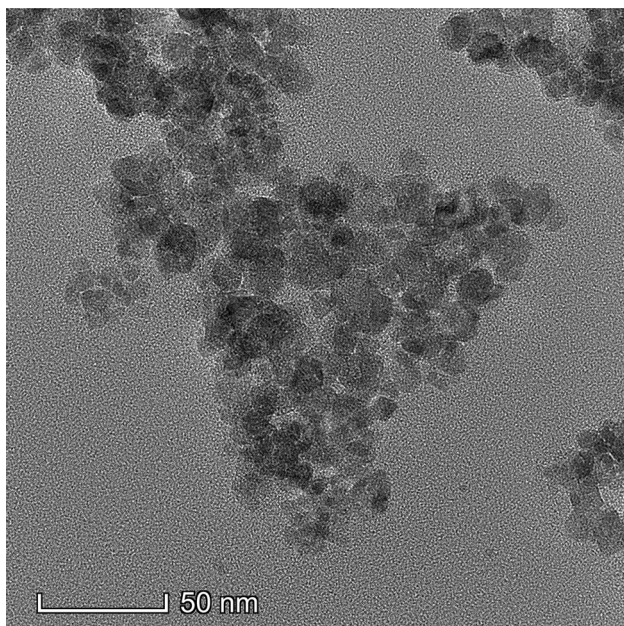
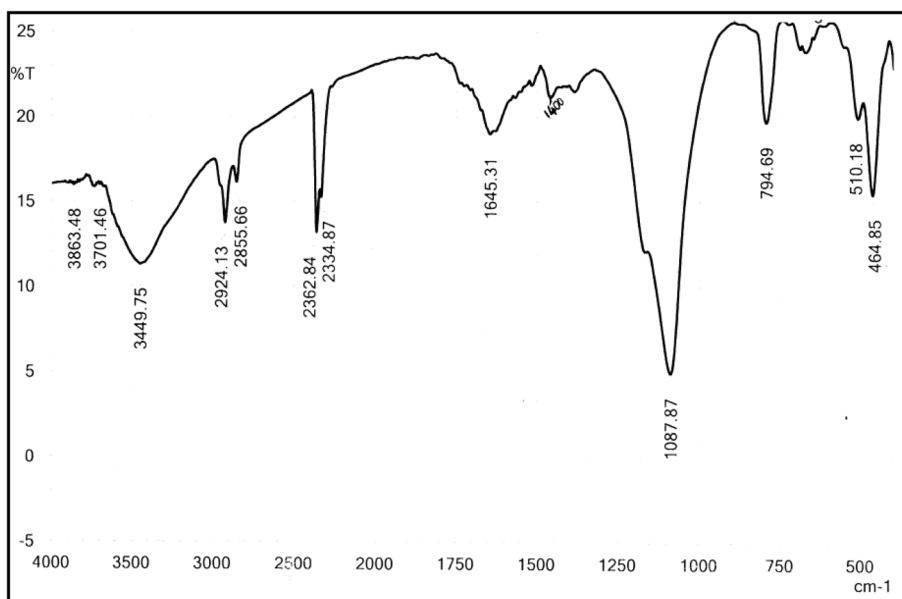


Fig. 4 XRD pattern of the synthesized silver nanoparticles

responsible for the reduction of  $\text{Ag}^+$  ions and stabilization of AgNPs. Figure 5 shows the FT-IR spectra of the synthesized AgNPs incorporated with the bio-molecules of *C. nucifera* in the wavenumbers range of  $400\text{--}4000 \text{ cm}^{-1}$ . Three strong peaks appeared at  $3450$ ,  $1645$  and  $1089 \text{ cm}^{-1}$  in the spectrum of synthesized AgNPs that are responsible for the stretching vibration of  $\text{--OH}$ ,  $\text{--C=O}$  and  $\text{C--O--C}$  bonds, respectively [1, 14, 67]. The weak peaks appeared at  $1400$ ,  $2855$  and  $2924 \text{ cm}^{-1}$  were due to the stretching vibration bands of  $\text{C--N}$  of the amine,  $\text{N--H}$  and  $\text{C--H}$ , respectively [1, 14, 96]. The weak and sharp peak centered at  $2363$  and  $2335 \text{ cm}^{-1}$ , respectively correspond to the stretching and bending vibration of the  $\text{C=O}$  bond within  $\text{CO}_2$  molecule, erupts during drying of AgNPs in addition to atmospheric  $\text{CO}_2$  [97]. The band at  $795 \text{ cm}^{-1}$  is indicative of the presence of heterocyclic compounds such as alkaloids [63]. The medium intense band at  $510 \text{ cm}^{-1}$  indicates the availability of aliphatic bromides [72]. The band at  $465 \text{ cm}^{-1}$  is due to Ag metal [5]. The FT-IR results indicate that the functional groups such as  $\text{C--N}$  of the amine,  $\text{--OH}$  and  $\text{N--H}$  present in the *C. nucifera* leaf extract is probably the responsible factors for the conversion of  $\text{Ag}^+$  ions to the metallic silver ( $\text{Ag}^0$ ) nanoparticles and act as the major capping agents accountable for the enhanced stability of the synthesized AgNPs and prevent agglomeration of the nanoparticles in the medium [1, 92]. Moreover, heterocyclic compounds such as alkaloids, flavones and anthracenes may also function as the capping agent for AgNPs [67]. Other biological molecules such as proteins can also bind silver nanoparticle either through free amine or cysteine groups in proteins to enhance the function for the formation and stabilization of the AgNPs in aqueous medium [98, 99]. The amino acid residues, carbonyl groups, and peptides also have a strong

**Fig. 5** FT-IR spectrum of the synthesized silver nanoparticles using *C. nucifera* leaf extract



**Fig. 6** TEM image of the synthesized silver nanoparticles

tendency to bind the AgNPs and acts as a capping agent [99, 100].

### 3.1.4 Surface Morphological Studies by Transmission Electron Microscope (TEM)

The TEM image of the synthesized AgNPs (Fig. 6) depicts a relatively spherical shape with the size below 20 nm and uniform distribution of the particles over the surface with almost no agglomeration. This less agglomeration of the

AgNPs might be attributed to the encapsulation of NPs with a thick layer of biomolecules indicating the potentiality of *C. nucifera* leaf extract. The TEM image depicted that the AgNPs were assembled onto the surface and are probably due to the several interactions such as Van der Waals and electrostatic interactions between the bioorganic capping molecules and AgNPs [94]. The NPs were not in direct contact even inside the aggregates, implying the stabilization of NPs by the capping agents [94, 101].

### 3.1.5 Antibacterial Activity of the Synthesized AgNPs

The antibacterial activity of the synthesized AgNPs was investigated against two Gram-positive bacteria viz., *S. aureus* and *B. subtilis*, and four Gram-negative bacteria viz., *S. typhimurium*, *E. coli*, *P. aeruginosa* and *C. freundii* using the standard disc diffusion method. Figure 7 shows the zones of inhibition produced by the AgNPs against the tested microorganisms. The zones of inhibition  $\pm$  standard deviation for *S. aureus*, *B. subtilis*, *S. typhimurium*, *E. coli*, *P. aeruginosa*, and *C. freundii* bacteria were obtained to be around  $12 \pm 0.06$ ,  $10 \pm 0.05$ ,  $13 \pm 0.12$ ,  $16 \pm 0.11$ ,  $19 \pm 0.06$  and  $20 \pm 0.12$  mm, respectively. Each value of the zone of inhibition is the rounded mean value of three replicate measurements of the inhibition diameter (mm) in the bacterial layer. The zone of inhibition was measured after incubating the strains for 24 h at 37 °C in the agar medium. The pictorial representations and the comparison of the values of the antibacterial activity of the synthesized AgNPs are shown in Figs. 7 and 8, respectively. Table 1 summarized the comparison of the antibacterial activities of the green synthesized AgNPs with the literature.



**Fig. 7** Zone of inhibition of (1) deionized water, (2) leaf extract and (6) AgNPs against Gram-positive bacteria: *Staphylococcus aureus* (S.A.) and *Bacillus subtilis* (B.S.); and Gram-negative bacteria: *Salmonella typhimurium* (S.T.), *Escherichia coli* (E.C.), *Pseudomonas aeruginosa* (P.A.), and *Citrobacter freundii* (C.F.)

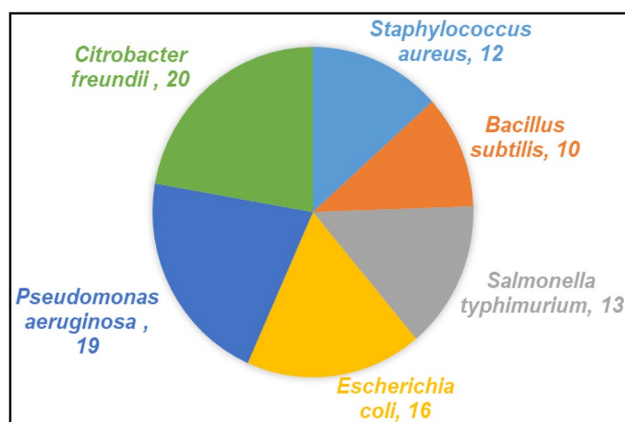
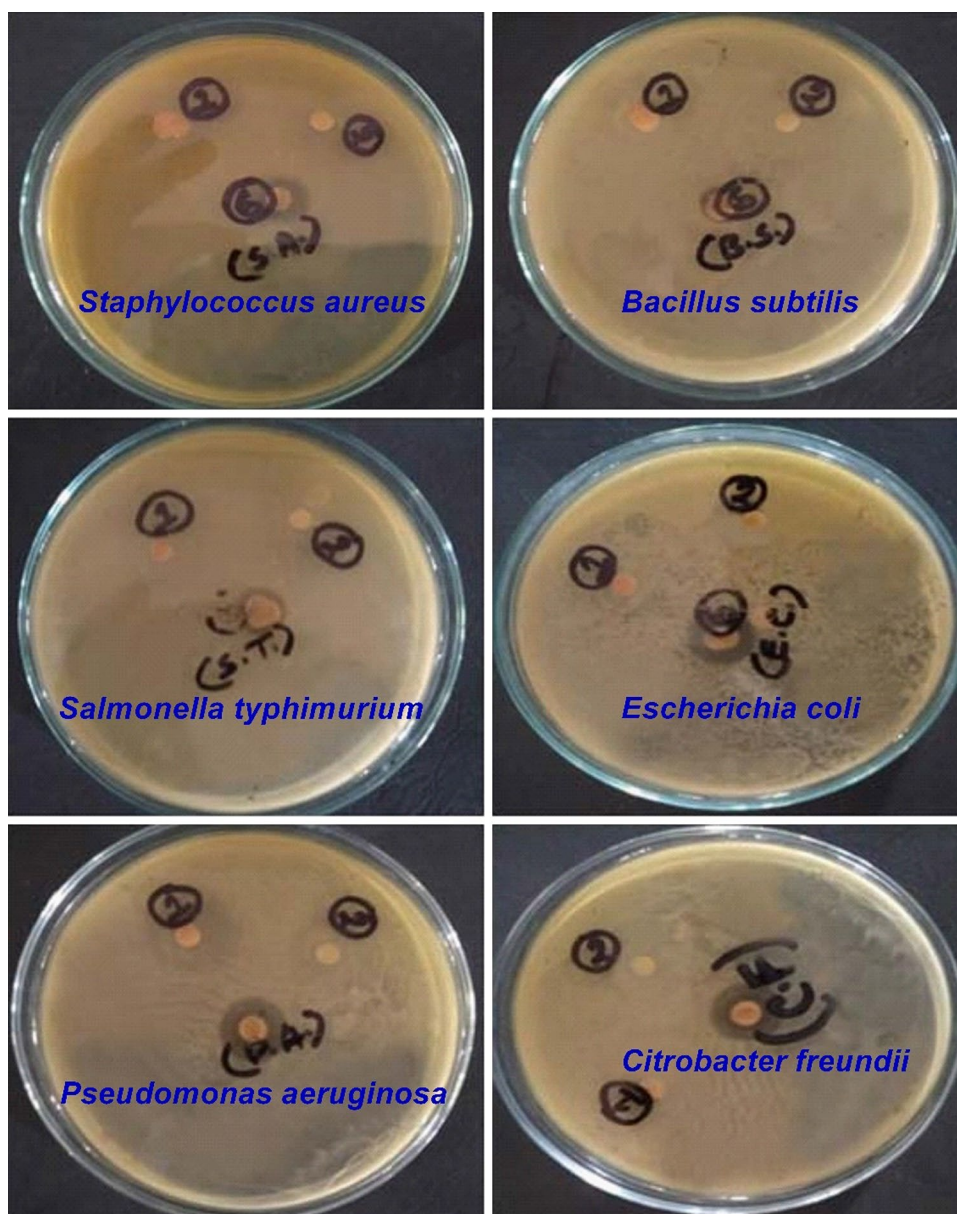


**Fig. 8** Antimicrobial activities of the synthesized AgNPs against the considered microorganisms (values are in mm)

The antibacterial activity was expressed in term of the diameter of the zone of inhibition and <9 mm zone was considered as inactive; 9–12 mm as partially active; while 13–18 mm as active and > 18 mm as very active [71]. The results demonstrated that the synthesized AgNPs showed considerable inhibition against both the Gram-positive and Gram-negative bacteria. However, the material showed less inhibition against Gram-positive bacteria than those of Gram-negative bacteria (Fig. 7) and this could be attributed to the thicker and rigid multiple cell layers of peptidoglycan of Gram-positive bacteria which prevent the penetration of AgNPs, and other toxins and chemicals into the cell wall [55, 104]. No zones of



**Table 1** Comparison of the zones of inhibition produced by the various green synthesized AgNPs against pathogenic bacteria

Studied bacteria	Biosource of extract	Size of AgNPs (nm)	AgNPs concentration (mg/L)	Inhibition zones (mm)	References	Standard		
						a	b	
<i>S. aureus</i>	<i>Chrysanthemum indicum</i> (flower)	52	25	8.33	[61]	8	8.12	
	<i>Cocous nucifera</i> (inflorescence)	22	100	0.00	[71]			
	Orange peel	98.43	100	10.0	[5]			
	<i>Melissa officinalis</i>	12–15	100	6.00	[102]			
	<i>Phlomis</i>	19–30	100	14.7	[55]			
	<i>Aloe vera</i>	10–30	50	18.1	[103]			
	<i>Lepidium draba</i>	20–80	100	10.8	[52]			
	<i>Eriobotrya japonica</i>	20–50	100	4.50	[53]			
	<i>Artocarpus heterophyllus</i>	13–15	100	15.0	[1]			
	<i>C. nucifera</i> (leaf)	14.2	30	12.0±0.06	This work			
<i>B. subtilis</i>	<i>Chrysanthemum indicum</i> (flower)	52	25	0.00	[61]	11	13.2	
	<i>Cocous nucifera</i> (inflorescence)	22	100	14.0	[71]			
	<i>C. nucifera</i> (leaf)	14.2	30	10.0±0.05	This work			
<i>S. typhimurium</i>	<i>Helicteres isor</i>	16–95	100	9.00	[102]	–	–	
	<i>Phlomis</i>	19–30	100	14.9	[55]			
	<i>Aloe vera</i>	10–30	50	6.30	[103]			
	<i>Lepidium draba</i>	20–80	100	10.4	[52]			
	<i>Artocarpus heterophyllus</i>	13–15	100	18.0	[1]			
	<i>C. nucifera</i> (leaf)	14.2	30	13.0±0.12	This work			
		<i>Chrysanthemum indicum</i> (flower)	52	12.5	3.00			[61]
<i>E. coli</i>	<i>Cocous nucifera</i> (inflorescence)	22	100	12.0	[71]			
	Orange peel	98.43	100	21.0	[5]			
	<i>Helicteres isor</i>	16–95	100	4.00	[102]			
	<i>Phlomis</i>	19–30	100	15.1	[55]			
	<i>Eriobotrya japonica</i>	19.75	100	2.50	[53]			
	<i>Melissa officinalis</i>	12	100	5.00	[51]			
	<i>Lepidium draba</i>	20–80	100	10.8	[52]			
	<i>Ocimum Sanctum</i>	10–20	150	14.0	[50]			
	<i>Artocarpus heterophyllus</i>	13–15	100	19.0	[1]			
	<i>Fagonia indica</i> (callus)	–	400	12.0	[3]			
	<i>C. nucifera</i> (leaf)	14.2	30	16.0±0.11	This work			
	<i>P. aeruginosa</i>	<i>Chrysanthemum indicum</i> (flower)	52	37.5	9.60	[61]	10	14.1
		<i>Cocous nucifera</i> (inflorescence)	22	100	14.0	[71]		
<i>C. nucifera</i> (leaf)		14.2	30	19.0±0.06	This work			
<i>C. freundii</i>	<i>Piper nigrum</i> (leaf)	7–50	100	8.96	[6]	–	–	
	<i>Piper nigrum</i> (stem)	9–30	100	8.89	[6]			
	<i>C. nucifera</i> (leaf)	14.2	30	20.0±0.12	This work			

<sup>a</sup>Ampicilin (10 mg/mL) [71]

<sup>b</sup>Streptomycin (25 mg/L) [61]

inhibition for the DI water and leaf extract as the negative control were observed against the tested microorganisms. Although the exact mechanism of the antibacterial activity of the AgNPs against the studied human pathogens are still unknown and demand much depth study [59, 105], the catalytic activity and good penetrating capability of

the NPs into the bacterial cells affecting the bacterial membranes and their DNA replication may be the probable reason for their enhanced antimicrobial activities [29, 106].

## 4 Conclusions

Herein, we have successfully conducted the green synthesis of AgNPs using *C. nucifera* leaf extract as the natural reducing and stabilizing agent in a facile, precise, fast and efficient manner at room temperature and atmospheric pressure which was non-toxic, eco-friendly, and cost-effective. The formation of the desired AgNPs was confirmed by physical and instrumental techniques such as UV–Vis spectrophotometry, FT-IR, XRD, and TEM analyses. The material showed the characteristic absorption maxima at 380 nm in UV–Vis spectrum. The crystal phase of AgNPs as identified and confirmed from XRD analysis was a cubic structure with an average crystallite size of 14.2 nm. The synthesized AgNPs demonstrated potential antibacterial activity against both the Gram-positive (*S. aureus* and *B. subtilis*) and Gram-negative (*S. typhimurium*, *E. coli*, *P. aeruginosa*, and *C. freundii*) bacteria. The results of the antibacterial study clearly indicate that the newly synthesized AgNPs are promising antimicrobial agents against the considered pathogens. These might have immense and potential applications in biomedical, pharmaceutical, food and cosmetic industries, and could open an alternative door to chemically synthesized AgNPs.

**Acknowledgements** The authors are grateful to the Department of Chemistry, Comilla University, Bangladesh and BCSIR, Dhaka, Bangladesh for providing laboratory facilities and other logistic support during the research period. We are also grateful to Aminul Islam Chowdhury, Lecturer, Department of Applied Chemistry and Chemical Engineering, Faculty of Science, University of Chittagong, Bangladesh for providing the English language editing service.

**Author Contributions** AKMRU designed the experiment. FR carried out the laboratory synthesis of the material and prepare them for various analyses. MABS characterized the material, interpreted the analytical results, and drafted the manuscript. AKMAU and RK revised the manuscript critically for important intellectual content. All authors read and approved the final manuscript.

**Funding** The authors received no specific funding for this research work from elsewhere and the work is also not supported by or under any financing projects.

## Compliance with Ethical Standards

**Conflict of interest** The authors declare that they have no conflict of interest.

## References

1. A.K.M.A. Ullah, M.F. Kabir, M. Akter, A.N. Tamanna, A. Hossain, A.R.M. Tareq, M.N.I. Khan, A.F. Kibria, M. Kurasaki, M.M. Rahman, RSC Adv. **8**, 37176–37183 (2018)
2. S. Maiti, D. Krishnan, G. Barman, S.K. Ghosh, J.K. Laha, Anal. Sci. Technol. **5**, 40 (2014)
3. M. Adil, T. Khan, M. Aasim, A.A. Khan, M. Ashraf, AMB Expr. **9**, 75 (2019)
4. H. Padalia, P. Moteriya, S. Chanda, Arab. J. Chem. **8**, 732–741 (2015)
5. M.A. Awad, W.K. Mekhamer, N.M. Merghani, A.A. Hendi, K.M. Ortashi, F. Al-Abbas, N.E. Eisa, J. Nanomater. **2015**, 5 (2015)
6. K. Paulkumar, G. Gnanajobitha, M. Vanaja, S. Rajeshkumar, C. Malarkodi, K. Pandian, G. Annadurai, Sci. World J. **2014**, 9 (2014)
7. D.V. Parikh, T. Fink, K. Rajasekharan, N.D. Sachinvala, A.P.S. Sawhney, T.A. Calamari, A.D. Parikh, Text. Res. J. **75**, 134–138 (2005)
8. T. Dutta, A.P. Chattopadhyay, M. Mandal, N.N. Ghosh, V. Mandal, M. Das, J. Inorg. Organomet. Polym. Mater. (2019). <https://doi.org/10.1007/s10904-019-01332-8>
9. S. Ahmed, M. Ahmad, B.L. Swami, S. Ikram, J. Adv. Res. **7**, 17–28 (2016)
10. L. Huang, Y. Sun, S. Mahmud, H. Liu, J. Inorg. Organomet. Polym. Mater. (2019). <https://doi.org/10.1007/s10904-019-01313-x>
11. M. Popescu, A. Velea, A. Lorinczi, Dig. J. Nanomater. Bios. **5**(4), 1035–1040 (2010)
12. B. Baruwati, V. Polshettiwar, R.S. Varma, Green Chem. **11**, 926–930 (2009)
13. K.A. Willets, R.P. Van Duyne, Annu. Rev. Phys. Chem. **58**, 267–297 (2007)
14. M. Akter, M.M. Rahman, A.K.M.A. Ullah, M.T. Sikder, T. Hosokawa, T. Saito, M. Kurasaki, J. Inorg. Organomet. Polym. Mater. **28**, 1483–1493 (2018)
15. Q. Sun, X. Cai, J. Li, M. Zheng, Z. Chen, C.P. Yu, Colloids Surf. A **444**, 226–231 (2014)
16. P.L. Nadworny, J. Wang, E.E. Tredget, R.E. Burrell, J. Inflamm. **7**, 13 (2010)
17. K.J. Kim, W.S. Sung, B.K. Suh, S.K. Moon, J.S. Choi, J.G. Kim, D.G. Lee, Biometrics **22**, 235–242 (2009)
18. R.O. Becker, Met.-Based Drugs. **6**, 311–314 (1999)
19. H. Barani, J. Inorg. Organomet. Polym. Mater. (2019). <https://doi.org/10.1007/s10904-019-01335-5>
20. S. Gajbhiye, S. Sakharwade, J. Cosmet. Dermatol. Sci. Appl. **6**, 48–53 (2016)
21. M. Akter, M.T. Sikder, M.M. Rahman, A.K.M.A. Ullah, K.F.B. Hossain, M. Kurasaki, J. Adv. Res. **9**, 1–16 (2018)
22. Z. Shavandi, T. Ghazanfari, K.N. Moghaddam, Immunopharmacol. Immunotoxicol. **33**, 135–140 (2011)
23. J.H. Sung, J.H. Ji, J.D. Park, J.U. Yoon, D.S. Kim, K.S. Jeon, Toxicol. Sci. **108**, 452–461 (2009)
24. A. Angelova, B. Angelov, Neural Regen. Res. **12**(6), 886–889 (2017). <https://doi.org/10.4103/1673-5374.208546>
25. M.P. Patil, R.D. Singh, P.B. Koli, K.T. Patil, B.S. Jagdale, A.R. Tipare, G.-D. Kim, Microb. Pathog. **121**, 184 (2018)
26. S. Pirtarighat, M. Ghannadnia, S. Baghshahi, J. Nanostruct. Chem. **9**(1), 1–9 (2019)
27. S.R. Modi, J.J. Collins, D.A. Relman, J. Clin. Investig. **124**, 4212–4218 (2014)
28. K. Paul, B.G. Bag, K. Samanta, Appl. Nanosci. **4**, 769–775 (2014)
29. G.A. Martinez-Castanon, N. Nino-Martinez, F. Martinez-Gutierrez, J.R. Martinez-Mendoza, F. Ruiz, J. Nanopart. Res. **10**, 1343–1348 (2008)
30. F. Mafune, J.Y. Kohno, Y. Takeda, T. Kondow, H. Sawabe, J. Phys. Chem. B **104**, 9111–9117 (2000)
31. B. Wiley, Y. Sun, B. Mayers, Y. Xia, Chemistry **11**, 454–463 (2005)

32. M.M. Oliveira, D. Ugarte, D. Zanchet, A.J. Zarbin, J. Colloid Interface Sci. **292**, 429–435 (2005)
33. G. Merga, R. Wilson, G. Lynn, B.H. Milosavljevic, D. Meisel, J. Phys. Chem. C **111**, 12220–12226 (2007)
34. N. Roy, A. Barik, Int. J. Nanotechnol. Appl. **4**, 95–101 (2010)
35. F. Cheng, J.W. Betts, S.M. Kelly, J. Schaller, T. Heinze, Green Chem. **15**, 989–998 (2013)
36. J. Li, Q. Wu, J. Wu, *Handbook of Nanoparticles* (Springer, Berlin, 2015), pp. 1–28
37. Y.F. Li, W.P. Gan, Z.H.O.U. Jian, Z.Q. Lu, Y.A.N.G. Chao, T.T. Ge, Trans. Nonferrous Met. Soc. China **25**(6), 2081–2086 (2015)
38. M. Mohammadlou, H. Jafarizadeh-Malmiri, H. Maghsoudi, Green Process. Synth. **6**(1), 31–42 (2017)
39. K. Byrappa, M. Yoshimura, *Handbook of Hydrothermal Technology* (William Andrew, Norwich, 2001)
40. J. Zou, Y. Xu, B. Hou, D. Wu, Y. Sun, China Particuol. **5**(3), 206–212 (2007)
41. R. Geethalakshmi, D.V.L. Sarada, Int. J. Nanomed. **7**, 5375–5384 (2012)
42. B. Ankamwar, C. Damle, A. Ahmad, M. Sastry, J. Nanosci. Nanotechnol. **5**, 1665–1671 (2005)
43. A.K. Mishra, K.N. Tiwari, R. Saini, P. Kumar, S.K. Mishra, V.B. Yadav, G. Nath, J. Inorg. Organomet. Polym. Mater. (2019). <https://doi.org/10.1007/s10904-019-01392-w>
44. H.D. Beyene, A.A. Werkneh, H.K. Bezabh, T.G. Ambaye, Sustain. Mater. Technol. **13**, 18–23 (2017)
45. M.S. Kiran, V.S. Betageri, C.R. Kumar, S.P. Vinay, M.S. Latha, J. Inorg. Organomet. Polym. Mater. (2020). <https://doi.org/10.1007/s10904-020-01443-7>
46. R. Seifipour, M. Nozari, L. Pishkar, J. Inorg. Organomet. Polym. Mater. (2020). <https://doi.org/10.1007/s10904-020-01441-9>
47. A. Shehzad, M. Qureshi, S. Jabeen, R. Ahmad, A.H. Alabdallal, M.A. Alfajary, E. Al-Suhaimi, PeerJ **6**, 6086 (2018)
48. J.S. Moodley, S.B.N. Krishna, K. Pillay, P. Govender, Adv. Nat. Sci. Nanosci. Nanotechnol. **9**, 015011 (2018)
49. S.M. Ghaffoori, M. Entezari, A. Taghva, Z. Tayebi, Adv. Nat. Sci. Nanosci. Nanotechnol. **8**, 045019 (2017)
50. S. Jain, M.S. Mehata, Sci. Rep. **7**, 15867 (2017)
51. Á. de Jesús Ruíz-Baltazar, S.Y. Reyes-López, D. Larrañaga, M. Estévez, R. Pérez, Results Phys. **7**, 2639–2643 (2017)
52. F. Benakashani, A. Allafchian, S.A.H. Jalali, Green Chem. Lett. Rev. **10**, 324–330 (2017)
53. B. Rao, R.C. Tang, Adv. Nat. Sci. Nanosci. Nanotechnol. **8**, 015014 (2017)
54. A. Saravanakumar, M.M. Peng, M. Ganesh, J. Jayaprakash, M. Mohankumar, H.T. Jang, Artif. Cells Nanomed Biotechnol. **45**, 1165–1171 (2017)
55. A.R. Allafchian, S.Z. Mirahmadi-Zare, S.A.H. Jalali, S.S. Hashemi, M.R. Vahabi, J. Nanostruct. Chem. **6**, 129–135 (2016)
56. G.A. Nasir, A.K. Mohammed, H.F. Samir, Iraqi J. Biotechnol. **15**, 12 (2016)
57. K. Anandalakshmi, J. Venugobal, V. Ramasamy, Appl. Nanosci. **6**, 399–408 (2016)
58. Y.Y. Mo, Y.K. Tang, S.Y. Wang, J.M. Lin, H.B. Zhang, D.Y. Luo, Mater. Lett. **144**, 165–167 (2015)
59. M.J. Ahmed, G. Murtaza, A. Mehmood, T.M. Bhatti, Mater. Lett. **153**, 10–13 (2015)
60. M.M. Khalil, E.H. Ismail, K.Z. El-Baghdady, D. Mohamed, Arab. J. Chem. **7**, 1131–1139 (2014)
61. S. Arokiyaraj, M.V. Arasu, S. Vincent, N.U. Prakash, S.H. Choi, Y.K. Oh, K.C. Choi, K.H. Kim, Int. J. Nanomed. **9**, 379 (2014)
62. M. Khan, M. Khan, S.F. Adil, M.N. Tahir, W. Tremel, H.Z. Alkhatlan, A. Al-Warthan, M.R.H. Siddiqui, Int. J. Nanomed. **8**, 1507 (2013)
63. K.P. Kumar, W. Paul, C.P. Sharma, Process Biochem. **46**, 2007–2013 (2011)
64. R. Sathyavathi, M.B. Krishna, S.V. Rao, R. Saritha, D.N. Rao, Adv. Sci. Lett. **3**, 138–143 (2010)
65. S.S.K. Kamal, P.K. Sahoo, J. Vimala, M. Premkumar, S. Ram, L. Durai, Acta Chim. Slov. **57**, 808–812 (2010)
66. D. Jain, H.K. Diama, S. Kachhwaha, S.L. Kothari, Dig. J. Nanomater. Biostruct. **4**, 557–563 (2009)
67. J. Huang, Q. Li, D. Sun, Y. Lu, Y. Su, X. Yang, H. Wang, Y. Wang, W. Shao, N. He, J. Hong, Nanotechnology **18**, 105104 (2007)
68. S. Li, Y. Shen, A. Xie, X. Yu, L. Qiu, L. Zhang, Q. Zhang, Green Chem. **9**, 852–858 (2007)
69. M. Beldjilali, K. Mekhissi, Y. Khane, W. Chaibi, L. Belarbi, S. Bousalem, J. Inorg. Organomet. Polym. Mater. (2019). <https://doi.org/10.1007/s10904-019-01361-3>
70. M.N. Raj, D.R.K. Arulmozhi, Int. J. Sci. Res. Dev. **2**, 10 (2014)
71. R. Mariselvam, A.J.A. Ranjitsingh, A.U.R. Nanthini, K. Kalirajan, C. Padmalatha, P.M. Selvakumar, Spectrochim Acta Part A **129**, 537–541 (2014)
72. M. Govarthanan, Y.S. Seo, K.J. Lee, I.B. Jung, H.J. Ju, J.S. Kim, M. Cho, S. Kamala-Kannan, B.T. Oh, Artif. Cells Nanomed. Biotechnol. **44**, 1878–1882 (2016)
73. M. Gomathi, A. Prakasam, R. Chandrasekaran, G. Gurusubramaniam, K. Revathi, S. Rajeshkumar, J. Clust. Sci. **30**, 1–8 (2019)
74. S.M. Roopan, G. Madhumitha, A.A. Rahuman, C. Kamaraj, A. Bharathi, T.V. Surendra, Ind. Crops Prod. **43**, 631–635 (2013)
75. P.J. Babu, R.K. Das, A. Kumar, U. Bora, Int. J. Green Nanotechnol. **3**, 13–21 (2011)
76. E.K. Elumalai, K. Kayalvizhi, S. Silvan, J. Pharm. Bioallied Sci. **6**, 241 (2014)
77. P.K. Ghosh, P. Bhattacharjee, S. Mitra, M. Poddar-Sarkar, Int. J. Food Sci (2014). <https://doi.org/10.1155/2014/310852>
78. C. Imo, C.S. Ezeonu, N.G. Imo, C.J. Anigbo, Asian. J. Biochem. **13**, 9–14 (2018)
79. E.B.C. Lima, C.N.S. Sousa, L.N. Menezes, N.C. Ximenes, S. Júnior, G.S. Vasconcelos, N.B.C. Lima, M.C.A. Patrocínio, D. Macedo, S.M.M. Vasconcelos, Brazilian J. Med. Biol. Res. **48**, 953–964 (2015)
80. H.F. Wertheim, D.C. Melles, M.C. Vos, W. van Leeuwen, A. van Belkum, H.A. Verbrugh, J.L. Nouwen, Lancet Infect. Dis. **5**, 751–762 (2005)
81. L. Rhayat, M. Maresca, C. Nicoletti, J. Perrier, K.S. Brinch, S. Christian, E. Devillard, E. Eckhardt, Front. Immunol. **10**, 564 (2019)
82. A. Fabrega, J. Vila, Clin. Microbiol. Rev. **26**, 308–341 (2013)
83. S.C.L. Edberg, E.W. Rice, R.J. Karlin, M.J. Allen, J. Appl. Microbiol. **88**, 106S–116S (2000)
84. S.A. Evans, S.M. Turner, B.J. Bosch, C.C. Hardy, M.A. Woodhead, Eur. Respir. J. **9**, 1601–1604 (1996)
85. G. Davies, A.U. Wells, S. Hoffman, S. Watanabe, R. Wilson, Eur. Respir. J. **28**, 974–979 (2006)
86. P.L. Ho, K.N. Chan, M.S. Ip, W.K. Lam, C.S. Ho, K.Y. Yuen, K.W. Tsang, Chest **114**, 1594–1598 (1998)
87. A.Y. Bhagirath, Y. Li, D. Somayajula, M. Dadashi, S. Badr, K. Duan, BMC Pulm. Med. **16**, 174 (2016)
88. A. Joaquin, S. Khan, N. Russell, N. Al Fayed, Pediatr. Neurosurg. **17**, 23–24 (1991)
89. P.R. Murray, B. Holmes, H.M. Aucken, *Topley & Wilson's Microbiology and Microbial Infection* (Edward Arnold Ltd., London, 2010)
90. O. Prakash, R. Kumar, A. Mishra, R. Gupta, Pharmacogn. Rev. **3**, 353 (2009)
91. X.F. Zhang, Z.G. Liu, W. Shen, S. Gurnathan, Int. J. Mol. Sci. **17**, 1534 (2016)
92. J.M. Ashraf, M.A. Ansari, H.M. Khan, M.A. Alzohairy, I. Choi, Sci. Rep. **6**, 20414 (2016)



93. M. Sastry, K.S. Mayya, K. Bandyopadhyay, *Colloids Surf. A* **127**, 221–228 (1997)
94. M.M. Priya, B.K. Selvi, J.A.J. Paul, *Dig. J. Nanomater. Biostruct.* **6**, 869–877 (2011)
95. Y.H. Hsueh, K.S. Lin, W.J. Ke, C.T. Hsieh, C.L. Chiang, D.Y. Tzou, S.T. Liu, *PLoS ONE* **10**, e0144306 (2015)
96. Y. Yamamoto, T. Miura, M. Suzuki, N. Kawamura, H. Miyagawa, T. Nakamura, K. Kobayashi, T. Teranishi, H. Hori, *Phys. Rev. Lett.* **93**, 116801 (2004)
97. D.P. Dubal, D.S. Dhawale, R.R. Salunkhe, C.D. Lokhande, *J. Electrochem. Soc.* **157**, A812–A817 (2010)
98. A. Gole, C. Dash, V. Ramachandran, S.R. Sainkar, A.B. Mandale, M. Rao, M. Sastry, *Langmuir* **17**, 1674–1679 (2001)
99. N. Golla, J. Avilala, M.A. Alzohairy, H. Khadri, M. Koduru, *Int. J. Nano Dimens.* **4**, 77–83 (2013)
100. D.S. Balaji, S. Basavaraja, R. Deshpande, D. Bedre Mahesh, B.K. Prabhakar, A. Venkataraman, *Colloids Surf. B* **68**, 88–92 (2009)
101. J.Y. Song, B.S. Kim, *Korean J. Chem. Eng.* **25**, 808–811 (2008)
102. S. Bhakya, S. Muthukrishnan, M. Sukumaran, M. Muthukumar, *Appl. Nanosci.* **6**, 755–766 (2016)
103. T.A. Abalkhil, S.A. Alharbi, S.H. Salmen, M. Wainwright, *Biotechnol. Biotechnol. Equip.* **31**, 411–417 (2017)
104. F. Okafor, A. Janen, T. Kukhtareva, V. Edwards, M. Curley, *Int. J. Environ. Res. Public Health.* **10**, 5221–5238 (2013)
105. M.R. Bindhu, M. Umadevi, *Spectrochim. Acta Part A* **128**, 37–45 (2014)
106. S.J. Klaine, P.J. Alvarez, G.E. Batley, T.F. Fernandes, R.D. Handy, D.Y. Lyon, S. Mahendra, M.J. McLaughlin, J.R. Lead, *Environ. Toxicol. Chem.* **27**, 1825–1851 (2008)

**Publisher's Note** Springer Nature remains neutral with regard to jurisdictional claims in published maps and institutional affiliations.